

# Simulation of 3D periodic piezoelectric transducers radiating in layered media using Finite Element/Boundary element Analysis

Sylvain BALLANDRAS<sup>1</sup>, Raphaël LARDAT<sup>2</sup>, Mikaël WILM<sup>3</sup>, Alexandre REINHARDT<sup>4</sup>,  
Thomas PASTUREAUD<sup>2</sup>, Vincent LAUDE<sup>1</sup>, William DANIAU<sup>1</sup>, Raphaël ARMATI<sup>1</sup>,  
William STEICHEN<sup>2</sup>, Olivier BURAT<sup>5</sup>

<sup>1</sup> Institut FEMTO-ST, UMR CNRS 6174, Département LPMO, Besançon, France

<sup>2</sup> TEMEX SA, Sophia Antipolis, France

<sup>3</sup> LUSSE, FRE CNRS 2448, Tours, France

<sup>4</sup> Department of Physics, University of Bath, Bath, United Kingdom

<sup>5</sup> FRAMATOME-ANP, Saint-Marcel, France

**Abstract.** This paper is devoted to the description of a mixed finite element/boundary element analysis for the simulation of any periodic transducer radiating in any combination of solid and fluids assuming flat interfaces and linear operation regime. The theoretical developments required in that purpose are described and different examples of transducers are considered to demonstrate the interest of the proposed approach.

## 1. Introduction

Acoustic probes based on ultrasound transducers are now very standard tools for medical diagnostics and non-destructive evaluation [1,2]. Technological developments in this field during tens of years have yielded the production of very sensitive acoustic probes providing accurate measurements for a wide range of applications. Such technical improvements are also due to a strong effort in modelling the dynamical behaviour of these transducers [3,4,5]. However, the need of optimised acoustic transducer for the development of high quality imaging probes still requires efficient simulation tools providing reliable descriptions of the behaviour of real devices.

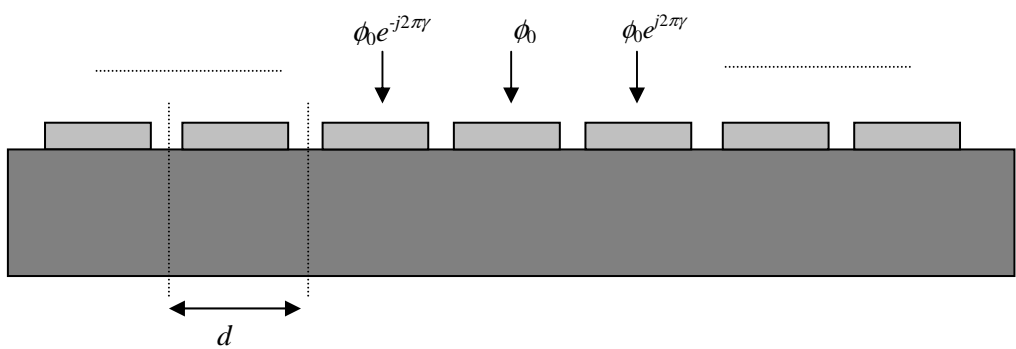
The basic design of piezoelectric transducers requires calculation tools that are able to accurately simulate complex arrangements of materials exhibiting acoustic and dielectric losses [6], together with a reliable representation of acoustic radiation in fluids [7]. As a more advanced requirement, the periodicity of the probes needs to be taken into account [8]. This is compulsory to correctly predict their capability to convert efficiently bulk vibrations into acoustic radiation, but also to quantitatively evaluate any parasitic effect due to wave guiding along the array's surface [9]. We present a mixed finite element /boundary element computation tool developed to address these problems. It is based on an harmonic analysis of any transducer simulated by finite element analysis (FEA) combined with boundary element methods (BEM) to simulate acoustic radiation in different media assuming plane interfaces [10,11]. Periodicity is taken into account using a standard periodic finite element approach [8, 12] and a Bloch-Floquet expansion for the radiation medium. This later can be composed of any combination of dielectric, metallic and fluid

media, taking into account acoustic, piezoelectric and dielectric losses for solids as well as viscosity for fluids [13], assuming flat interfaces between the different layers. Computations are performed for different kinds of piezoelectric and capacitive ultrasonic transducers to illustrate the proposed approach. The computation of actual radiated acoustic field can be computed taking advantage of the derivation of mutual terms deduced from the harmonic analysis by Fourier transform. This approach is described and illustrated for typical transducer configurations (1 and 2D periodic arrays).

## 2. Fundamentals

### 2.1 Harmonic excitation

The fundamentals of the harmonic excitation assumption for periodic systems has been published numerous times [14,15,16]. In this section, we briefly recall the aim of this approach, pointing out the basic hypotheses and their consequences on the physical data and parameters considered in our models. In the usual harmonic excitation assumptions, we consider that harmonic quantities are computed and then the corresponding mutual values are deduced from these data by Fourier transform. In that matter, depending on the nature of the addressed problem, we consider a harmonic excitation (for instance the force  $F$ , or electrical potential  $\phi$ ) governed by the following form, as illustrated in fig.1 :

$$F_n = F_o e^{-j2\pi n} \quad \phi_n = \phi_o e^{-j2\pi n} \quad (1)$$


The diagram shows a series of rectangular transducers on a substrate. Three downward arrows represent harmonic excitation at different phases:  $\phi_0 e^{-j2\pi\gamma}$ ,  $\phi_0$ , and  $\phi_0 e^{j2\pi\gamma}$ . A double-headed arrow below the substrate indicates the distance  $d$  between two adjacent transducers.

Fig. 1 – Definition of the harmonic excitation boundary condition.

In Eq.(1),  $n$  refers to the cell number and  $\gamma$  is the excitation coefficient [16]. Considering those excitation forms, it is possible to derive a parameter independent on the cell number, usually called harmonic admittance ( $\tilde{Y}$ ) or impedance ( $\tilde{Z}$ ) in the case of piezoelectric devices and for which an equivalent can be derived for purely mechanical problems too [16]. Considering  $I$  and  $V$  as the harmonic current and potential difference applied to the transducer, these parameters are defined as

$$\frac{V_n}{I_n} = \tilde{Z}(\gamma) = \sum_{n=-\infty}^{+\infty} Z_n e^{-j2\pi n\gamma} \leftrightarrow \frac{I_n}{V_n} = \tilde{Y}(\gamma) = \sum_{n=-\infty}^{+\infty} Y_n e^{-j2\pi n\gamma} \quad (2)$$

According to the classical Fourier theory, the weight of these infinite series developments  $Y_n$  or  $Z_n$  can be deduced from their harmonic equivalent by inverse Fourier transform, yielding the definition of mutual quantities as follows

$$Z_n = \int_0^1 \tilde{Z}(\gamma) e^{j2\pi n\gamma} d\gamma \quad Y_n = \int_0^1 \tilde{Y}(\gamma) e^{j2\pi n\gamma} d\gamma \quad (3)$$

As it is shown further, those relations apply for spectral and time domain analysis as well. The advantages related to both approaches are commented in the section devoted to numerical applications.

## 2.2 Finite element formulation

Figure 2 shows a general scheme of the considered periodic device geometry. Periodicities are assumed taking place in the plane  $(x_1, x_2)$ . The corresponding periods are noted  $d_1$  and  $d_2$ . The transducer is assumed inhomogeneous along  $x_3$ , imposing to mesh the corresponding region. It can be composed of various materials with arbitrary shapes assuming they can be well represented using an elastic displacement (and if required electrical potential) based FEA formulation. Material losses can also be considered by assuming complex elastic, piezoelectric and dielectric coefficients [6].

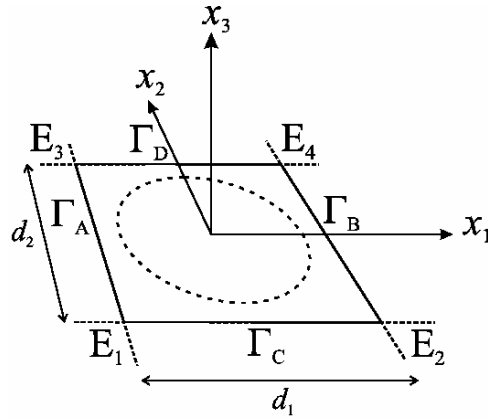


Fig. 2 – Axes and notation conventions used to represent a 2D periodic structure.

The basic equations governing periodic FEA computations are now briefly recalled. As already reported in previous references [8,12], FEA can be performed for periodic devices with rather simple modifications of the basic algebraic formula relating the displacement and electrical fields to the boundary solicitations. In the case of 2D periodicity devices, it first consists in relating all the degrees of freedom (dof) on boundaries in regards, i.e.  $\Gamma_A$  with  $\Gamma_B$  and  $\Gamma_C$  with  $\Gamma_D$ , and those on the corners of the mesh noted  $E_1$  to  $E_4$  in Fig. 2, yielding the following expressions first proposed in ref. [8]

$$\begin{aligned}
 u_{\Gamma_B} &= u_{\Gamma_A} e^{-j2\pi\gamma_1} \\
 u_{\Gamma_D} &= u_{\Gamma_C} e^{-j2\pi\gamma_2} \\
 u_{E_2} &= u_{E_1} e^{-j2\pi\gamma_1} \\
 u_{E_3} &= u_{E_1} e^{-j2\pi\gamma_2} \\
 u_{E_4} &= u_{E_1} e^{-j2\pi(\gamma_1+\gamma_2)}
 \end{aligned} \tag{4}$$

in which  $u$  holds for the generalized displacements (including the electrical potential), and  $\gamma_1$  and  $\gamma_2$  are the excitation parameters lying respectively along  $x_1$  and  $x_2$ . This relation is then used to reduce the number of independent dof of the FEA model. This is performed without changing the total number of dof of the problem, simply by using a variable change operator  $C$  that depends on the excitation parameter  $\gamma$ . Note that relation (4) does not depend on the kind of FEA performed and can be applied for linear analysis in harmonic, modal and transient regimes as well [17]. For harmonic and modal analyses, the FEA system to solve reads

$${}^t[C^*(\gamma_1, \gamma_2)][K - \omega^2 M][C(\gamma_1, \gamma_2)]\{v\} = {}^t[C^*(\gamma_1, \gamma_2)]\{F\} \tag{5}$$

where  $K$  is the stiffness matrix,  $M$  is the mass matrix,  $F$  is the external solicitation vector (Neumann boundary conditions) and  $v$  is the new set of independent dof. The operator  $C$  is a triangular complex matrix. If  $K$  is complex (i.e. accounting for material losses), the matrix product in (5) results in a general complex matrix with no particular properties. In the piezoelectric case, those matrices are generalized (i.e. accounting also for the electrostatic energy equilibrium) and  $M$  then is singular.

In the case of modal analysis of piezoelectric devices, Eq.(5) is used with the right hand side set to zero to compute the eigenvalues and eigenvectors thanks to a generalized algorithm based on the so-called QZ approach proposed by Moler and Stewart [18]. For general harmonic boundary conditions problems, the system is solved using a general linear solver dedicated to sparse complex matrices [19]. For transient analysis, the Newmark integration scheme is adopted since it complies with the acoustic equation requirements (2<sup>nd</sup> order problems) and because of its absolute stable behavior [20]. The corresponding matrix formulation is reported below, showing how the periodicity is accounted for in that particular case.

$${}^t[C^*(\gamma_1, \gamma_2)] [A_q] [C(\gamma_1, \gamma_2)] \{v_{n+q}\} = {}^t[C^*(\gamma_1, \gamma_2)] \left\{ \Delta t^2 \sum_{i=0}^q \beta_i \{F_{n+q}\} - [A_{q-1}] \{v_{n+q-1}\} - [A_{q-2}] \{v_{n+q-2}\} - \dots \right\} \quad (6)$$

with  $(\alpha_q [M] + \Delta t \gamma_q [L] + \Delta t^2 \beta_q [K]) = [A_q]$  and  $L$  accounts for visco-elastic losses (assuming no relaxation effects). In this equation,  $q$  represents the iteration number of the integration scheme (2 in the present case). Along that approach, the system to solve is factorised once using for instance a general Gauss method (or better, a method dedicated to hermitian matrices), and the solution for each iteration  $\Delta t$  then is computed thanks to the factorised system, what considerably saves time.

### 2.3 Radiation boundary conditions

The accurate simulation of a transducer operation requires accounting for realistic boundary conditions, particularly when estimating parameters such as bandwidth, sensitivity, directionality, cross-talks and so on. Efforts have been deployed in that purpose, taking advantage of all the developments achieved in geophysics to well understand the capability of acoustic sources to launch energy within semi-infinite or stratified media [21]. In the following developments, we show how radiation conditions can be accounted for in the periodic FEA we have introduced in the previous section. We use the concept of BEM built using the Green's function of the radiation media assuming of course linearity but also rigid baffle conditions (well adapted to a formulation in displacement and potential) and plane radiation surfaces. Green's functions are a useful concept used to represent numerically the response to applied stresses of a medium or of a stratified structure. In practice, they are defined as the linear relationship relating displacements and stresses at a given radiating surface. Along this approach, almost any kind of stratified radiation media can be simulated, composed of any combination of fluids and solids, taking viscosity and material losses into account [10,11,13]. One can relate the dynamic stress  $T_{ij}$  to the displacement  $u_k$  in the spectral domain and in the real domain as follows

$$\begin{aligned}\tilde{T}_{ij} &= \tilde{G}_{ijk}(s, \omega) \tilde{u}_k \leftrightarrow T_{ij} = G_{ijk}(r, t) * u_k \\ \tilde{u}_i &= \tilde{g}_{ijk}(s, \omega) \tilde{T}_{jk} \leftrightarrow u_i = g_{ijk}(r, t) * T_{jk}\end{aligned}\quad (7)$$

where  $s$  denote the slowness vector,  $r$  the real coordinates vector and  $*$  the convolution operation. Note that  $\tilde{G}$  asymptotically behaves like  $s$  when  $s$  tends to infinity whereas  $\tilde{g}$  exhibit a  $1/s$  asymptotic behaviour, meaning than the latter is holomorph in the integration domain (excepted at its poles). As a counterpart,  $\tilde{G}$  does not exhibit any pole but is not holomorph. Practically for spectral harmonic FEA-based models, this does not generate any numerical trouble. Equation (7) allows one for considering any flat boundary for the application of the radiation conditions, even if tilted in the radiation plane. Using the now well-established periodic Green's function formalism [22], we show how the radiation condition impacts on the external solicitation term of the elastic Lagrangian.

$$\begin{aligned}\iint_{\Gamma} \delta u_i^* T_{ij} n_j dS &= \\ \frac{n_j}{d_1 d_2} \iint_{\Gamma} \delta u_i^*(x_1, x_2) \sum_{k, l=-\infty}^{+\infty} G_{ijk}(\gamma_1 + k, \gamma_2 + l, \omega) \times & \\ e^{-j\frac{2\pi}{d_1}(\gamma_1+l)(x_1-x_1')} e^{-j\frac{2\pi}{d_2}(\gamma_2+l)(x_2-x_2')} u_k(x_1', x_2') dx_1' dx_2' dx_1 dx_2 &\end{aligned}\quad (8)$$

with  $k$  and  $l$  the numbers of the current space harmonics. The classical FEA interpolation procedure then is applied to (8). The computation of the radiation contribution via the development of (8) always converges even for large number of space harmonics. Practically, we have pointed out an optimum between the number of radiating elements and the space harmonics allowing for a systematic convergence.

The contribution of the total radiating boundary to the global algebraic system to be solved consists then in a frequency and excitation parameter dependent matrix  $X(\omega, \gamma)$  related to both dof and variational unknowns and consequently computed in the left hand side of (2) as reported in the following equation describing a general piezoelectric problem

$$\begin{bmatrix} C_u^*(\gamma) & 0 \\ 0 & C_\phi^*(\gamma) \end{bmatrix} \left( \begin{bmatrix} K_{uu} & -\omega^2 M_{uu} & K_{u\phi} \\ & K_{\phi u} & K_{\phi\phi} \end{bmatrix} - \begin{bmatrix} X_{uu}(\omega, \gamma) & X_{u\phi}(\omega, \gamma) \\ X_{\phi u}(\omega, \gamma) & X_{\phi\phi}(\omega, \gamma) \end{bmatrix} \right) \begin{bmatrix} C_u(\gamma) & 0 \\ 0 & C_\phi(\gamma) \end{bmatrix} \begin{Bmatrix} v \\ \phi \end{Bmatrix} = \begin{bmatrix} C_u^*(\gamma) & 0 \\ 0 & C_\phi^*(\gamma) \end{bmatrix} \begin{Bmatrix} F \\ Q \end{Bmatrix} \quad (9)$$

For materials exhibiting losses, this algebraic system is general complex without any specific mathematical characteristics. Also the sparse nature of the algebraic system is degraded due to the connection of all the dof of the radiating boundaries one to the other via the radiation coupling.

In the time and real space domains, the Green's function is much more difficult to establish than in the spectral (frequency and wave-number) domain. For semi-infinite fluid media, it is possible (see for instance [1] and [23]) to derive both 2D and 3D Green's function relating the pressure to the displacement normal to the radiating surface, as reported below

$$\begin{aligned}g(t, r) &= 0 \text{ for } t < rs_f \\ g(t, r) &= \frac{1}{2\pi\sqrt{t^2 - (rs_f)^2}} \text{ in 2D for } t > rs_f \quad g(t, r) = \frac{\delta(t - rs_f)}{4\pi r} \text{ in 3D for } t > rs_f\end{aligned}\quad (10)$$

with  $r = \sqrt{(x_1 - x_1')^2 + (x_2 - x_2')^2 + (x_3 - x_3')^2}$  and  $s_f$  the specific wave slowness in the fluid. The pressure  $p(X,t)$  ( $X$  is the coordinate vector) is then computed as a double convolution product in space and time as follows

$$p(X,t) = \rho_f \int_{\Gamma} \int_{\tau} \left( g(X, X', t, \tau) \frac{d^2 u_n(X', \tau)}{d\tau^2} \right) d\tau dS' \quad (11)$$

For semi-infinite solid media, there is no equivalent analytic expression allowing for an easy description of their impulse response, but it is possible to access the Green's function in space and time thanks to the very useful relation established by Hodé and Desbois [24] stating that the imaginary part of the spectral Green's function is equivalent to the real space and time Green's function because of their fundamental properties (the existence of a canonical form of the Green's function). The implementation of those equations is now under development.

### 3. Results

Many different structures have been considered for validating the proposed approach. We briefly report here the more representative ones, allowing to emphasize the nature of the analysis achievable using such computation tools. We will mainly focus on piezocomposite and micro-machined ultrasonic transducers (MUT) [25] allowing for very nice illustrations of our computing tool exploitation.

#### 3.1 2-2 Piezocomposite

An interesting validation of the periodic time domain analysis was achieved considering a 2-2 piezocomposite [17]. The structure of the device is shown in Fig. 3, consisting in a PZT/epoxy combination with a volume fraction of about 50%. The transducer is excited by applying a Dirac-like voltage on the top side, the bottom side being grounded. The current is computed for each periodic parameter  $\gamma$  on a sufficiently long time for a faithful representation of the device operation. The mutual currents (equivalent to the mutual admittance for a unitary excitation) are then deduced from the harmonic analysis, allowing to clearly identify cross-talks effects due to elastic coupling from one cell to another. These results are reported in Fig.4(a&b).

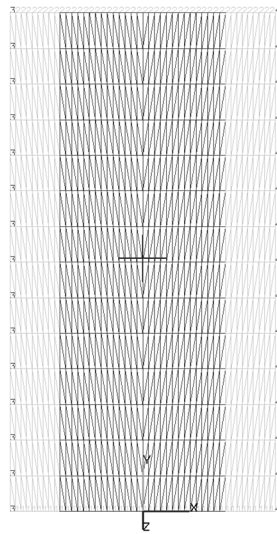


Fig. 3 – Mesh of the 2-2 connectivity piezocomposite (PZT : dark grey, Epoxy : light grey, bounds 3 and 4 coupled via periodicity conditions)

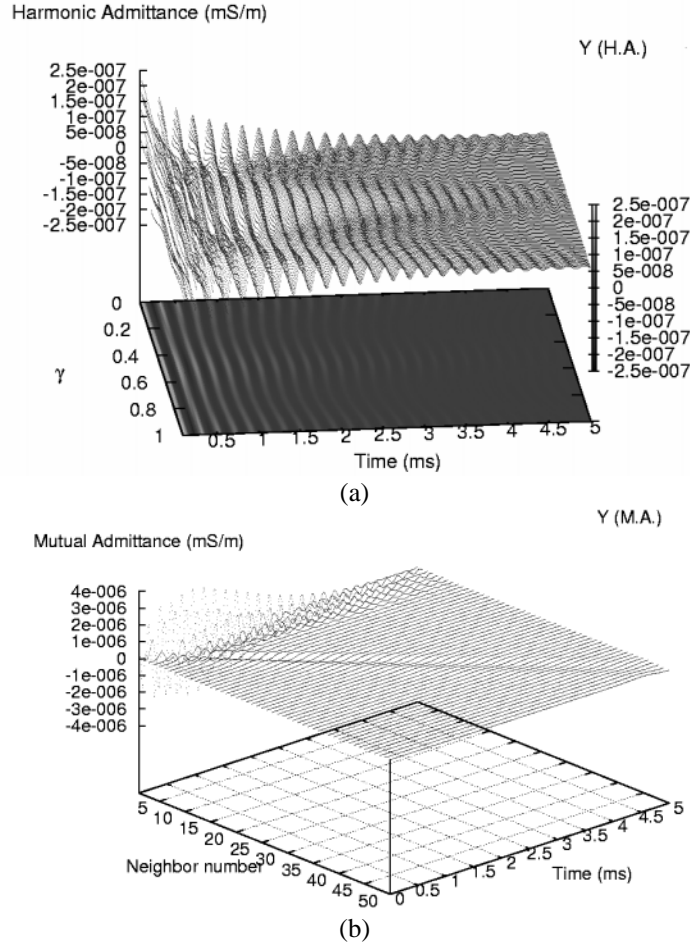


Fig. 4 – Harmonic admittance of the piezocomposite unit cell (a) and related mutual admittances of the 49 first neighbors

Figure 4(a) shows the total absence of singular behaviour of the current (admittance) even for a high quality factor device, allowing then for an easy derivation of the mutual terms since only simple numerical integration tools have to be implemented in that matter. Figure 4(b) is particularly interesting as it reveals the respect of causality by the absence of any signal before the arrival of the slowest wave guided by the array. One can then easily deduce the velocity of the slowest wave guided by the transducer and relate it to the corresponding Lamb-like mode.

### 3.2 Micro-machined Ultrasonic Transducers (MUTs)

In that case, we present an analysis of a capacitive MUT (c-MUT) in the spectral domain. First we report the result of the harmonic analysis, allowing for the identification of the different modes of the structure versus the excitation factor and taking into account radiation phenomena on the front side (water) and on the bottom side (silicon plate) as well. This is an illustration of a full 3D bi-periodic transducer radiating in fluids and solids as well. Such a computation can be also achieved for standard transducers (see for instance [26]). Figure 5 shows the mesh used for computations. 2<sup>nd</sup> degree interpolation polynomials were used to achieve the reported results. In that case, we excite the membrane of the structure assuming a unit force distributed on the inner side, varying the periodic parameter  $\gamma_1$  and fixing  $\gamma_2$  to zero. Figure 6 shows the corresponding mean normal displacement of the membrane loaded by water. The expected wide band response actually occurs for  $\gamma_1=0$ , but it is also pointed the existence of numerous modes guided at the interface between the membrane and the fluid, allowing for the definition of the mode diagram reported in Fig.7.

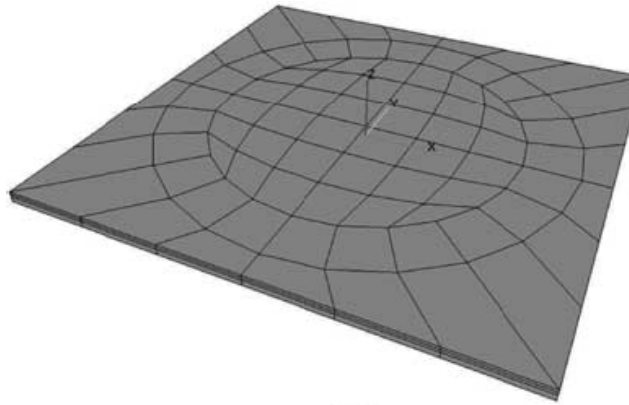


Fig.5 – Mesh implemented for the simulation of bi-periodic cMUT

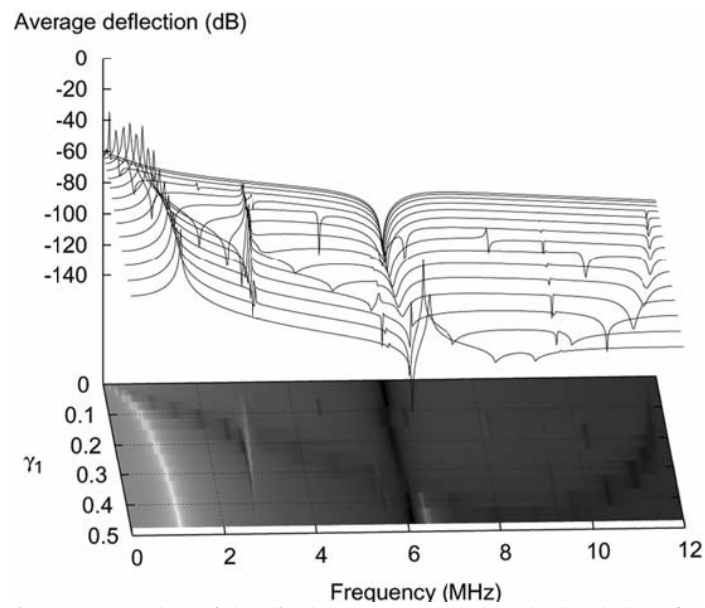


Fig.6 Mean value of the displacement normal to the loaded surface

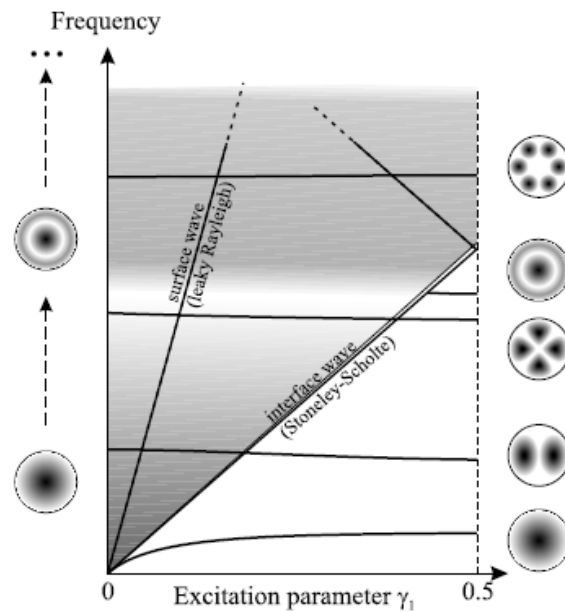


Fig.7 – Definition of the mode of the loaded membrane (the Wilm's diagram [27])

One can note that the harmonic analysis points out the existence of sharp responses due to guided waves at the liquid/solid interface. This generates difficulties in the extraction of mutual terms by Fourier transform. In this work, a numerical integration scheme has been adopted in that purpose. 30 integration points have been considered, allowing for computing the mutual displacements up to the 10<sup>th</sup> neighbor of the excited cell. This is enough for evaluating the cross-talk effects in the near neighboring, but clearly, to compute radiation figures such as those in Ref. [16], a higher precision is required, hence a higher number of integration points. Such problem won't occur anymore for time domain analyses, as shown in sect. 3.1

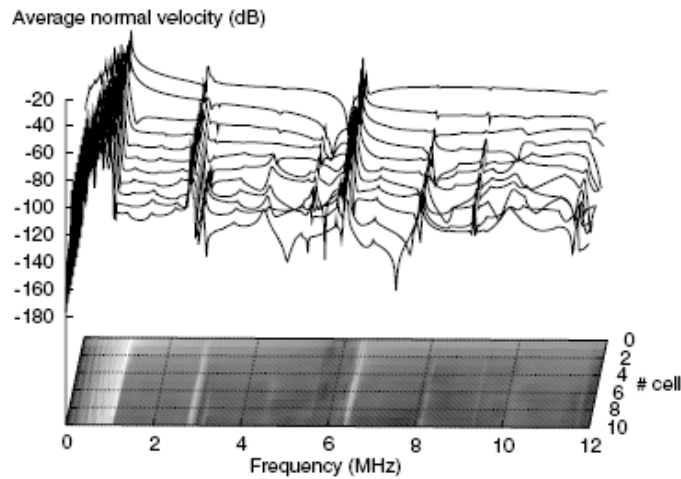


Fig.8 Mutual displacements of cMUTs radiating in water (front side) on semi-infinite silicon (back side)

## Conclusion

The development of numerical tools for the computation of ultrasound transducers response when in operation still requires numerous efforts, to fully understand the involved physical phenomena and to propose new approaches or strategies to improve their characteristics. We have shown how harmonic analyses can be used to allow for accessible computation duration when simulating or optimizing a periodic transducer. Different approaches can be implemented in that way, mixing BEM with FEA to accurately account for radiation conditions in different kind of media (mainly stratified or semi-infinite). Time domain computations appear as a promising tool to increase the level of analysis, including the simulation of non linear phenomena such as used in capacitive transducers or involved in large excitation regime (particularly for therapy purpose in medicine). On the other hand, it appears still limited for simulating radiations in complex media, even considering the simplified case of stratified domain (plane interface assumptions). A wise approach then consists in using those tools in a combinatory way, using first spectral computations for the evaluation of linear parameters (directivity, sensitivity, bandwidth, etc.) and time domain for adjusting the analysis, computing cross-talk phenomena and including non-linear properties when necessary. Future developments will be achieved along that scheme.

## Acknowledgements

The presented developments have been achieved thanks to the support of TEMEX and FRAMATOME-ANP.

## References

- [1] G. S. Kino, *Acoustic Waves, Devices, Imaging and Analog Signal Processing*, Prentice-Hall, Englewood Cliffs, NJ, (1987).
- [2] W.P. Mason editor, *Physical Acoustics, Principle and Methods*, Academic Press, New York, San Francisco, London, 1964.
- [3] H. Allik, T.J.R. Hugues, *Int. J. Num. Meth. Eng.* **2**, 151 (1970).
- [4] W. Steichen, G. Vanderbork, Y. Lagier, in *Power Sonics and Ultrasonics Trans. Des.*, 160 (1988).
- [5] R. Lerch, *IEEE. Trans. on UFFC*, **37**, 233 (1990).
- [6] S. Sherrit, B.K. Mukherjee, *Proc. of the IEEE Ultrasonics Symp., Sendai*, **1**, 633 (1998)
- [7] P.F. Edoa, S. Ballandras, M. Wilm, *J. Acoust. Soc. Am.*, **115**, 2947 (2004).
- [8] P. Langlet, A.C. Mladky-Hension, J.N. Decarpigny, *S. de Physique IV, Colloque C1*, **2** (1992).
- [9] X. Geng, Q.M. Zhang, *IEEE Trans. on UFFC*, **44**(4), 857 (1997)
- [10] T. Pastureaud, V. Laude, S. Ballandras, *Appl. Phys. Lett.* **80**, 2544 (2002).
- [11] A. Reinhardt, T. Pastureaud, S. Ballandras, V. Laude, *J. Appl. Phys.* **94**, 6923 (2003).
- [12] S. Ballandras, M.Wilm, P.F. Edoa, V. Laude, A. Soufyane, W. Steichen, R. Lardat, , *J. of Appl. Phys.*, **93**, 702 (2003).
- [13] S. Ballandras *et al.*, *J. Appl. Phys.* **99**, 054907 (2006).
- [14] Y. Zhang, J. Desbois, L. Boyer, *IEEE Trans. on UFFC*, **40**, 183 (1993)
- [15] J. Koskela, V. P. Plessky, and M. M. Salomaa, *IEEE Trans. on UFFC*, **45**, 439 (1998)
- [16] S. Ballandras, M. Wilm, J.F. Gelly, *IEEE Trans. on UFFC*, **53** (1), 209 (2006)
- [17] S. Ballandras, V. Laude, S. Clatot, M. Wilm, *Proc. of the IEEE Ultrasonics Symp.*, **1**, 337 (2005)
- [18] Moler, C., and G.W. Stewart (1973), *SIAM Journal on Numerical Analysis*, **10**, 241–256.
- [19] T.A. Davis, I. S. Duff, *SIAM J. Matrix Analysis and Applications*, **18**(1), 140 (1997)
- [20] O.C. Zienkiewicz, R. L. Taylor, J.Z. Zhu, *The Finite Element Method*, Elsevier Butterworth-Heinemann Ed., *6<sup>th</sup> Edition*, **1** (2005)
- [21] A. H. Fahmy, E. L. Adler, *Appl. Phys. Lett.* **22**, 495 (1973).
- [22] V. P. Plessky, Th. Thorvaldsson, *IEEE Trans. on UFFC*, **42**(2), 280 (1995)
- [23] J. Diaz, Thèse de Doctorat de l'Université de Paris VI, spécialité Mathématiques Appliquées, 2005
- [24] J.M. Hodé, J. Desbois, *Proc. of the IEEE Ultrasonics Symp.*, 131 (1999)
- [25] B.T. Khury-Yakub, F.L. Degertekin, X.C. Jin, S. Calmes, I. Ladabaum, S. Hansen, X.J. Zhang, *Proc. of the IEEE Ultrasonics Symp.*, 985 (1998)
- [26] S. Ballandras, M. Wilm, V. Laude, W. Daniau, F. Lanteri, J.-F. Gelly, O. Burat, R. Lardat and T. Pastureaud, *Proc. of the World Congress on Ultrasound, Paris*, 1553 (2003)
- [27] Mikaël Wilm, Alexandre Reinhardt, Vincent Laude, Raphaël Armati, William Daniau, Sylvain Ballandras, *Ultrasonics*, **43**, 457 (2005)